applied sciences

MDPI

Article

Transbulbar B-Mode Sonography for Clinical Phenotyping Multiple Sclerosis

Roberto De Masi [1,2,3,*], Stefania Orlando [1,2,4], Aldo Conte [2,3], Sergio Pasca [2,3], Rocco Scarpello [3], Pantaleo Spagnolo [5] and Antonella De Donno [4]

1 Laboratory of Neuroproteomics, Multiple Sclerosis Centre, "F. Ferrari" Hospital, 73042 Casarano, Italy; stephaniaorlando@gmail.com
2 Multiple Sclerosis Centre, "F. Ferrari" Hospital, 73042 Casarano, Italy; contealdo@tin.it (A.C.); sergio.pasca@virgilio.it (S.P.)
3 Complex Operative Unit of Neurology, "F. Ferrari" Hospital, 73042 Casarano, Italy; rocco.scarpello@gmail.com
4 Laboratory of Hygiene, Department of Biological and Environmental Sciences and Technologies, University of the Salento, 73100 Lecce, Italy; antonella.dedonno@unisalento.it
5 Division of Neuroradiology, "F. Ferrari" Hospital, 73042 Casarano, Italy; leospagnolo@gmail.com
* Correspondence: stefania.orlando@unisalento.it; Tel./Fax: +39-0833-508323

Received: 21 September 2018; Accepted: 2 November 2018; Published: 7 November 2018

Featured Application: Our data suggest a valuable role of B-mode sonography in the clinical phenotyping of MS patients. Given that therapeutic management of MS is closely related to subtype individuation, it follows that TBS could provide an objective instrumental criterion for personalized therapeutic choice in MS.

Abstract: The aim of this study was to assess putative differences in optic nerve sheath diameter (ONSD) and associated clinical/paraclinical variables between relapsing remitting (RR) and secondary progressive (SP) multiple sclerosis (MS) patients. We examined 60 relapse-free MS patients and 35 healthy controls by means of transbulbar B-mode sonography (TBS). Expanded disability status scale (EDSS) values were from 3 to 4 indicated patients with a transitional RR to SP phenotype. Mean ONSD was significantly lower in MS patients. Mean ONSD measured at 5 mm from the eyeball (ONSD5) was significantly lower in SP than in RR patients, while ONSD measured at 3 mm from the eyeball (ONSD3) was statistically higher in RR than in the transitional group. The myelination index (MI), i.e., the ratio of ONSD3 to ONSD5, was used to assess the relative myelination of the optic nerve (ON). Higher ONSD5 and MI (0.90) corresponded to patients with the RR phenotype having a mean EDSS of 2.0; lower MI (0.84) clustered the transitional patients having a mean EDSS of 3.7. Finally, lower MI with low ONSD3 identified the SP phenotype having a mean EDSS $\geq$ 4.0. The TBS in MS highlights chronic optic neuropathy, caused by early subclinical axonal loss and demyelination.

Keywords: high-resolution ultrasound; multiple sclerosis; optic nerve; transbulbar B-mode sonography

1. Introduction

Transbulbar B-mode sonography (TBS) has recently been standardized with reference to magnetic resonance imaging (MRI) for the reproducible and accurate study of the optic nerve (ON) in healthy controls and diseased subjects [1,2]. Since then, ultrasound imaging studies have identified a number of new pathological elements regarding other cranial nerves and peripheral trunks in many diseases, from optic neuritis and idiopathic intracranial hypertension (IIH) [3,4] to chronic idiopathic demyelinating polyneuropathy (CIDP) [5]. As regards multiple sclerosis (MS), the initial

findings showed that TBS was suitable for the study of the ON and its chronic and subclinical involvement in disease in form of ON atrophy, regardless of the degree of acute retrobulbar optic neuritis (ARON), which it also described [6,7]. Specifically, chronic ON atrophy has been demonstrated in unselected MS patients and optic nerve sheath diameter (ONSD) has also been correlated with neurological impairment detected by the expanded disability status scale (EDSS) [8]. However, the ON has never been studied selectively in the relapsing remitting (RR) and secondary progressive (SP) phenotypes of the disease and neither has ONSD in terms of the clinical or paraclinical variables of diseased subjects. Accordingly, we have not considered patients that experienced ARON in the past, for excluding the effect of acute inflammatory demyelination onto development of chronic ON atrophy, whose assessment is the main target of the present study.

The importance of studying the ON in MS lies in the certainty of its features that make it a good clinical model of the disease. First, the convergence of the ganglion cell output fibres in the ON makes it a clinically and instrumentally eloquent structure for all lesions [9]. Second, ON fibres are only unmyelinated in the lamina cribrosa, starting from the last 3 mm before their entry into the eyeball [10]. Therefore, we can study the thickness of the myelinated and unmyelinated parts of the ON (at 5 mm and 3 mm from the eyeball, respectively) under a range of experimental conditions. Third, its derivation from the diencephalon makes the ON sensitive to abiotrophic phenomena in distant structures of hemispheric white matter and the cortex [11,12]. Finally, we know the nature of subclinical histological processes leading to the end-stage atrophy of the ON in the large number of patients affected by MS. Specifically, common neuroinflammatory-dependent aspects involving the optic nerves and cerebral hemispheres include perivenular infiltrative T cells with axonal loss and reactive gliosis [13].

Based on this premise, the primary aim of this study is to assess putative differences in ONSD between RR and SP MS patients. A secondary aim is to evaluate which demographic, instrumental or clinical variables are associated with these differences among the MS study population. These data have a descriptive value since they constitute a novel application of the sonographic technique. However, they can also characterize sub-clinical disease progression in clinical practice.

2. Materials and Methods

In an unblinded, comparative, cross-sectional study, we investigated 41 (20 males, 21 females) relapse-free RRMS patients and 19 (8 males, 11 females) sex-matched SPMS patients and 35 (17 males, 18 females) healthy controls subjects, making a total of 95 eyes. We defined as "relapse-free" patients which are free from clinical (neurological worsening) or radiological (increasing MRI-detected lesion load) relapse by at least three months.

Given the negligible inter-side difference [8], the right eye of each subject was investigated by TBS as part of their clinical examination. Within 24 h, brain MRI was conducted and visual evoked potentials were measured among the MS group. Transbulbar B-mode sonography was carried out personally by the primary author of this work, a neurophysiologist certified by the Italian Neurosonology Society (Italian Society of Neurosonology and Brain Haemodynamics (SINSEC)). A GE Vivid 7 ultrasound system (GE Vingmed Ultrasound AS, Horten, Norway) was used in accordance with Bauerle et al. [1,2]. Briefly, with the 4–11 MHz linear probe placed on the temporal part of the closed upper eyelid, the optic nerve was depicted in a transverse plane, revealing the papilla and the optic nerve in its longitudinal course at 3 and 5 mm behind the eyeball bilaterally. The distance between the external borders of the hyperechoic area surrounding the ON was quantified as the ONSD.

P100 latency (P100L) and amplitude (P100A) were calculated in the right eye at a distance of 1 m from the checkboard, in accordance with Odom's pattern-reversal protocol. Briefly, full-field visual evoked potentials (VEPs) were extracted during 1 Hz alternating standard pattern stimulus on a high-contrast black and white chequerboard with a square element size of $1 \pm 20^{\circ}$ per side, after one hundred stimuli. Given that mean of P100L and P100A both exceeding significantly their normative

data, no healthy control group was planned. Specifically, values of 98.19 ± 0.75 ms and 7.23 ± 2.16 μv were used as normal cut-off for P100L and P100A, respectively [14].

All patients were positioned and imaged with a 1.5 T Philips MR apparatus (180 mT/m) (Achieva, Philips Medical Systems, Best, The Netherlands), in accordance with international guidelines [15]. SENSE (Sensitivity Encoding) parallel imaging method with contrast enhancement (Gadovist single dose, 10 min post-administration) was used. Modalities and acquisition sequence types are summarized in Table 1.

Table 1. Modalities and acquisition sequences of MRI (magnetic resonance imaging).

Parameter	Value
acquisition sequence	SE T1–TSE T1 MT–BRAIN VIEW FLAIR 3-D
acquisition time	2.17′–3.07′–4.14′
field of view	230 × 183 mm AX–250 FLAIR SAG–180 mm COR MT
orientation	TRA–COR–TRA
alignment	TRA–COR–TRA
voxel size	0.89/0.88/4–0.56/0.56/4–0.31/0.31/0.6
repetition time	450–614–4800
echo time	15–12–307
inversion time	/–/–1660
flip angle	69°–90°–/
number of excitation	1–2–2

The MRI post-analysis was conducted using "Sienax" software (Analysis Group, FMRIB, Oxford, UK) to determine brain parenchymal fraction (BPF), "MIPAV" (National Institutes of Health Center for Information Technology Rockville, MD, USA) to calculate the T1 and T2 lesion loads (T1LL, T2LL) and "SPM12" (Functional Imaging Laboratory, Wellcome Trust Centre for Neuroimaging, Institute of Neurology, London, UK) to calculate total brain volume (TBv), grey/white matter volume (GMv, WMv), CSF ventricular volume (CSFv), and peripheral grey matter volume (PGMv).

The clinical parameters considered were EDSS score and sub-scores and disease duration (DD). Developed by Kurtzke in 1983, the EDSS is a universal scale for quantifying neurological impairment in MS patients [16]. This method numerically quantifies overall disability with reference to the eight functional systems (pyramidal, sensitive, cerebellar, brain-stem, etc.) and allows neurologists to assign a functional system score (the so-called functional sub-score) to each of them. Co-morbidity, including ophthalmic and toxic-deficiency diseases, entailed exclusion from this study. Patients that relapsed three months before the study and those affected by retrobulbar optic neuritis were also excluded.

We also considered the ratio of ONSD at 3 mm from the eyeball (ONSD3) to ONSD at 5 mm from the eyeball (ONSD5), also called the myelination index (MI) [8]. We used the MI to associate knowledge of ONSD with the thickness of the myelin coating of the ON.

The Wilcoxon–Mann–Whitney test was applied to the difference between means. The ANOVA-associated K-means cluster analysis was used to determine the distribution and putative associations of MI and other variables among the MS patients. In addition, we used ROC analysis (Receiver operating characteristic curve) to determine the accuracy of each variable as an indicator of MS patient phenotype (RR or SP). The χ^2 test was used to verify the effective separation between the RR and SP groups, classifying patients with reference to an MI threshold value plus another clinical or paraclinical variable identified by the cluster analysis.

Finally, we used the coefficient of variation (COV) to determine the intra-observer reliability of ONSD, calculated on the basis of test-retest evaluations of the entire study population. Thus, every eyeball was examined twice, at the start of the study and 2–3 weeks after the first assessment. All subjects gave their informed consent for inclusion before they participated in the study. The study was conducted in accordance with the Declaration of Helsinki, and the protocol was approved by the Ethics Committee of A.S.L. LE (1057/DS).

3. Results

No statistical difference was found between the mean age of all MS patients (41.4 y; SD 2.5) and healthy controls (40.2 y; SD 1.78). Mean DD was 11.5 y (95% CI = 9.50–14.10); mean MI were 0.84 (95% CI = 0.83–0.89), and 0.89 (95% CI = 0.86–0.90), respectively.

Mean ONSD in patients at 3 and 5 mm from the eyeball was respectively 0.49 cm (95% CI = 0.45–0.52; SD 0.074) and 0.57 cm (95% CI = 0.55–0.60; SD 0.064). Mean ONSD in healthy controls at 3 and 5 mm from the eyeball was respectively 0.65 cm (95% CI = 0.62–0.68; SD 0.077) and 0.73 cm (95% CI = 0.70–0.78; SD 0.065). These differences between diseased patients and healthy subjects were highly significant. Specifically, at both 3 and 5 mm, the ONSD was found to be smaller in patients than in healthy controls ($p < 0.001$ in both cases).

The demographic and clinical features of all patients and healthy subjects are summarized in Table 2.

Table 2. Demographic and clinical characteristics of all MS (multiple sclerosis) patients and healthy controls [†].

Parameter	All MS Patients	Healthy Controls	*p*
N	60	35	
Age (y)	41.4 ± 2.5 [‡]	40.2 ± 1.8	
Female-to-male ratio	1.14	1.06	
Disease duration (y)	11.5 (9.50–14.10)	-	
Optic nerve sheath diameter (cm)			
At 3 mm	0.49 ± 0.074 (0.45–0.52)	0.65 ± 0.077 (0.62–0.68)	<0.001
At 5 mm	0.57 ± 0.064 (0.55–0.60)	0.73 ± 0.065 (0.70–0.78)	<0.001
Myelination index	0.84 (0.83–0.89)	0.89 (0.86–0.90)	<0.001

[†] Note that the optic nerve sheath diameter at both 3 and 5 mm was found to be lower in patients than in healthy controls patients ($p < 0.001$ in both cases). The Wilcoxon–Mann–Whitney test was applied to the difference between means. [‡] Values are given as the mean or mean ± standard deviation and, if necessary, with the 95% confidence interval in parentheses.

Statistical differences between RRMS and SPMS groups were found for mean age and DD. Specifically, the mean age was 39.5 y for RRMS patients (SD 7.9; 95% CI 36.4–42.2) and 46.7 y for SPMS patients (SD 8.1; 95% CI 41.2–51.7); mean DD was 10.0 y (SD 6.6; 95% CI 7.8–12.5) for RRMS patients and 15.8 y (SD 8.6; 95% CI 3.9–11.8) for SPMS patients. Mean EDSS was 2.2 (SD 0.8; 95% CI 1.9–2.5) in the RRMS group and 5.3 in the SPMS group (SD 0.7; 95% CI 4.8–5.7). The mean COV of ONSD was 0.065.

Mean ONSD in RR patients at 3 and 5 mm from the eyeball was respectively 0.51 cm (95% CI 0.48–0.53, SD 0.072) and 0.59 cm (95% CI 0.56–0.62, SD 0.081). Mean ONSD in SP patients at 3 and 5 mm from the eyeball was respectively 0.46 cm (95% CI 0.42–0.51, SD 0.077) and 0.55 cm (95% CI 0.51–0.58, SD 0.065). Specifically, at 5 mm, the ONSD was found to be smaller in SP patients than in RR patients ($p < 0.001$), but no significant difference was noted between the two groups at 3 mm ($p = 0.134$).

Considering the overall MS population, P100A and P100L correlated with the pyramidal EDSS sub-score as follows: $r = -0.37$; $p = 0.03$ and $r = 0.46$; $p = 0.007$, respectively (Figure 1).

The mean MI of the RR and SP groups was 0.86 (SD 0.083; 95% CI 0.85–0.88) and 0.83 (SD 0.11; 95% CI 0.76–0.87) respectively, the difference not being statistically significant ($p = 0.211$). The demographic and clinical/paraclinical features of RR and SP patients are summarized in Tables 3 and 4.

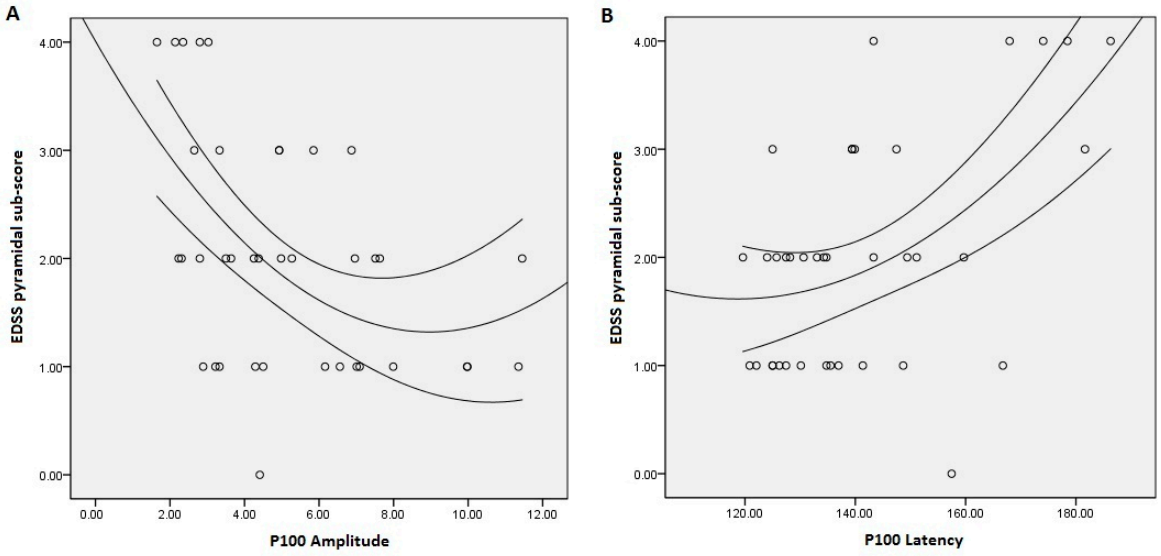

Figure 1. Correlation between P100 and EDSS (expanded disability status scale). (**A**) Significant inverse correlation between P100 Amplitude (μv) and EDSS pyramidal sub-score ($r = -0.37$; $p = 0.03$); (**B**) Significant direct correlation between P100 Latency (ms) and EDSS pyramidal sub-score ($r = 0.46$; $p = 0.007$). EDSS Expanded Disability Status Scale.

Table 3. Demographic and clinical characteristics of the study population [†].

Parameter	RR Patients	SP Patients	*p*
N	41	19	
Age (y)	39.5 ± 7.9 (36.4–42.2) [‡]	46.7 ± 8.1 (41.2–51.7)	0.008
Female-to-male ratio	1.05	1.37	
Disease duration (y)	10.0 ± 6.6 (7.8–12.5)	15.8 ± 8.6 (3.9–11.8)	0.050
Expanded Disability Status Scale	2.2 ± 0.8 (1.9–2.5)	5.3 ± 0.7 (4.8–5.7)	0.000
pyramidal sub-score	1.48 ± 0.64 (1.23–1.73)	3.36 ± 0.67 (3.00–3.75)	0.000
sensitive sub-score	1.04 ± 1.05 (0.63–1.43)	2.45 ± 0.82 (2.00–3.00)	0.000
cerebellar sub-score	0.18 ± 0.56 (0.00–0.41)	2.63 ± 0.50 (2.33–2.91)	0.000
brain-stem sub-score	0.37 ± 0.74 (0.12–0.68)	1.27 ± 1.27 (0.58–2.00)	0.046
sphincteric sub-score	0.15 ± 0.53 (0.00–0.37)	1.64 ± 1.21 (0.90–2.30)	0.002
Optic nerve sheath diameter (cm)			
At 3 mm	0.51 ± 0.072 (0.48–0.53)	0.46 ± 0.077 (0.42–0.51)	n.s.
At 5 mm	0.59 ± 0.081 (0.56–0.62)	0.55 ± 0.065 (0.51–0.58)	<0.001
Myelination index	0.86 ± 0.083 (0.85–0.88)	0.83 ± 0.11 (0.76–0.87)	n.s.

[†] Note that the optic nerve sheath diameter at 5 mm was found to be lower in SP patients than in RR patients. The Wilcoxon–Mann–Whitney test was applied to the difference between means. [‡] Values are given as the mean or mean ± standard deviation, with the 95% confidence interval in parentheses. RR Relapsing Remitting; SP Secondary progressive.

Statistical similarity analysis of the global population (RR + SP) blindly identified two clusters, one characterized by low MI ($MI^L = 0.84$) and another by high MI ($MI^H = 0.90$). The ANOVA found the distance between the variables' centres for the two groups to be statistically significant ($p = 0.050$).

Specifically, the MI^H group contained diseased subjects with high P100A and low P100L (respectively 6.36 μv and 136.09 ms), high PGMv and TBv (630,238.75 mm^3 and 1,558,847.53 mm^3), low T1LL and T2LL (respectively, 688.68 mm^3 and 2087.35 mm^3) and low age and DD (38.29 y and 8.36 y, respectively). This group included all the RR patients among the MS study population with a mean EDSS of 2.0.

The MI^L cluster included patients with low P100A and high P100L (respectively 4.06 μv and 146.25 ms), low PGMv and TBv (respectively 552,318.25 mm^3 and 1,447,772.14 mm^3), high T1LL and T2LL (respectively 5316.72 mm^3 and 11,128.67 mm^3) and high age and DD (45.47 y and 14.11 y, respectively).

This low MI group included the transitional phenotype patients among the MS study population having a mean EDSS of 3.7 and intermediate clinical and instrumental characteristics between the RR and SP groups. These intermediate clinical and instrumental characteristics are summarized in Table 5 as "Transitional", with values between those of RR patients in the same table and those of SP patients represented in Table 4.

Table 4. Paraclinical measurements of the study population †.

Parameter	RR Patients	SP Patients	*p*
T1 lesion load §	1577.23 ± 2261.02 ‡	6772.00 ± 6358.60	0.023
T2 lesion load	4158.20 ± 5299.07	13,916.02 ± 8143.61	0.003
BPF	0.9737 ± 0.1325	0.9623 ± 0.1328	0.045
GMv	763,145.65 ± 59,152.64	698,216.42 ± 47,061.52	0.004
WMv	759,098.84 ± 38,432.62	723,746.73 ± 44,805.69	0.032
CSFv	39,606.07 ± 18,441.77	53,428.45 ± 18,475.49	0.050
PGMv	599,272.76 ± 47,461.55	548,315.90 ± 35,203.95	0.003
TBv	1,522,244.48 ± 63,794.56	1,421,963.15 ± 29,322.82	0.000
P100 amplitude	5.84 ± 2.64 (4.82–6.90)	3.49 ± 1.66 (2.61–4.67)	0.003
P100 latency	135.39 ± 12.61 (130.80–140.38)	156.98 ± 21.05 (144.28–169.69)	0.007

† The Wilcoxon–Mann–Whitney test was applied to the difference between means. ‡ Values are given as the mean or mean ± standard deviation, with the 95% confidence interval in parentheses. § T1 lesion load, T2 lesion load, GMv, WMv, CSFv, PGMv and TBv are shown in mm^3; P100 amplitude is shown in μv; P100 latency is shown in ms. RR Relapsing Remitting; SP Secondary progressive; BPF Brain parenchymal fraction; GMv Grey Matter volume; WMv White matter volume; CSFv CSF ventricular volume; PGMv Peripheral grey matter volume; TBv Total brain volume.

The χ^2 test confirmed a significant difference between the frequencies of the MI^H (RR) and MI^L (transitional) patient groups. The centres of the clusters and their distances between groups are summarized in Table 5.

Table 5. Similarity statistical analysis with relapsing remitting and transitional groups characterization †.

	Cluster		
	High MI (Relapsing Remitting)	Low MI (Transitional)	*p* Value
MI	0.90	0.84	0.050
T1 lesion load (mm^3)	688.68	5316.72	0.004
T2 lesion load (mm^3)	2087.35	11,128.67	0.001
PGMv (mm^3)	630,238.75	552,318.25	0.000
TBv (mm^3)	1,558,847.53	1,447,772.14	0.000
P100 amplitude (μv)	6.36	4.06	0.006
P100 latency (ms)	136.09	146.25	0.050
Age (y)	38.29	45.47	0.010
Disease duration (y)	8.36	14.11	0.035
EDSS	2.0	3.7	0.001
ONSD3 (cm)	0.53	0.48	0.050

† Note that similarity statistical analysis blindly identified two clusters among the global population (RR + SP), one characterized by low MI ($MI^L = 0.84$) and another by high MI ($MI^H = 0.90$). ANOVA found the distance between the variables' centres in the two groups to be statistically significant ($p = 0.050$). The ANOVA-associated K-means cluster analysis was used to determine the distribution and putative associations of MI and other variables among the MS patients. The χ^2 test confirmed a significant difference between the frequencies of the MI^H and MI^L patient groups. MI Myelination Index; PGMv Peripheral grey matter volume; TBv Total brain volume; EDSS Expanded disability status scale. ONSD3 Optic nerve sheath diameter at 3 mm from the eyeball.

Finally, the ROC analysis highlighted the accuracy (good sensitivity and specificity) in classifying the MI^H and MI^L patients among the general population. The conviction strength of the test was statistically significant for EDSS ($p = 0.001$), T1LL ($p = 0.017$), T2LL ($p = 0.006$), PGMv ($p = 0.015$),

TBv (p = 0.000), P100L (p = 0.021), age (p = 0.050), and DD (p = 0.014), but not for MI (p = 0.059), as shown in Figure 2.

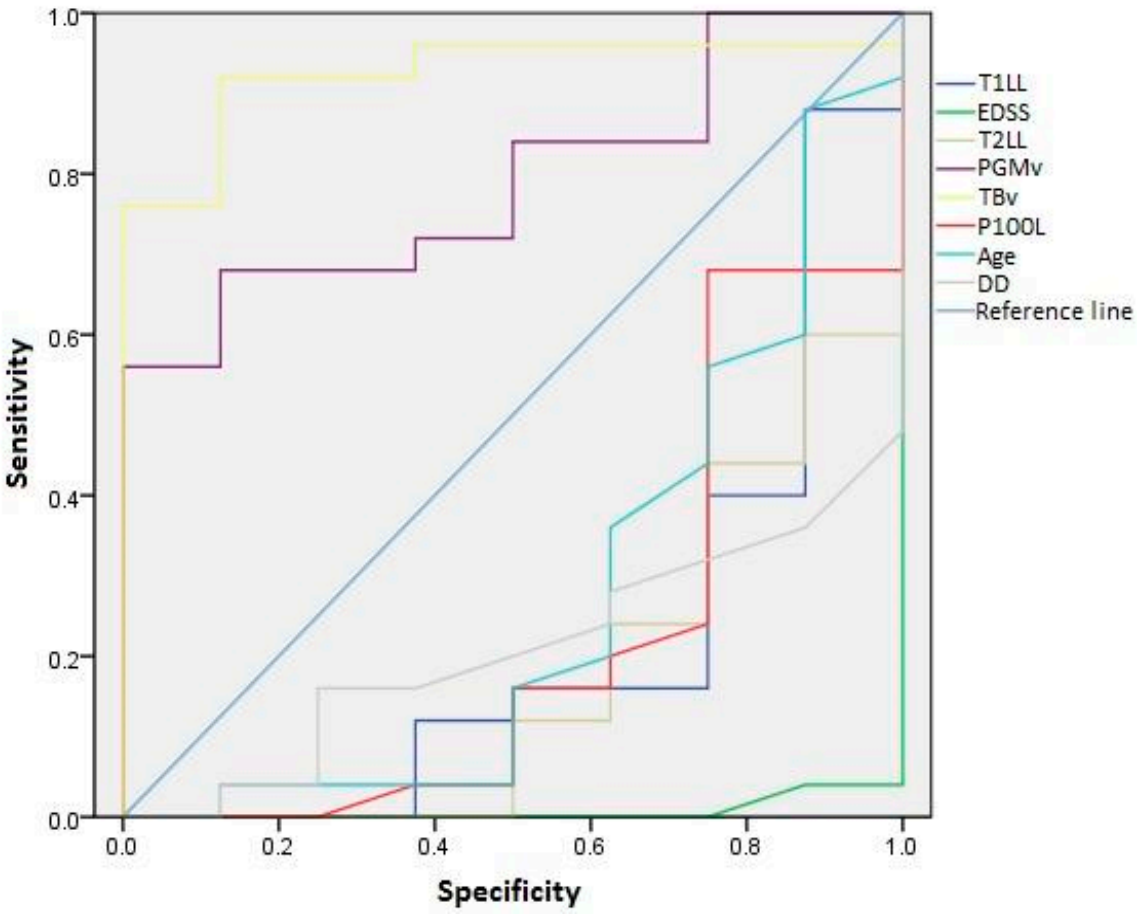

Figure 2. ROC analysis (Receiver operating characteristic curve). The ROC analysis highlighted the accuracy (good sensitivity and specificity) of the method in classifying MI^H and MI^L patients in the general population. The conviction strength of the test was statistically significant for EDSS (p = 0.001), T1LL (p = 0.017), T2LL (p = 0.006), PGMv (p = 0.015), TBv (p = 0.000), P100L (p = 0.021), age (p = 0.050), and DD (p = 0.014), but not for the MI (p = 0.059). EDSS Expanded disability status scale; T1LL T1 lesion load; T2LL T2 lesion load; PGMv Peripheral grey matter volume; TBv Total brain volume; P100L P100 latency; DD Disease duration; MI Myelination index; MI^H High myelination index; MI^L Low myelination index.

The MI correlated with ONSD3 (r = 0.499; p = 0.001), but not with the other clinical or paraclinical variables (Figure 3).

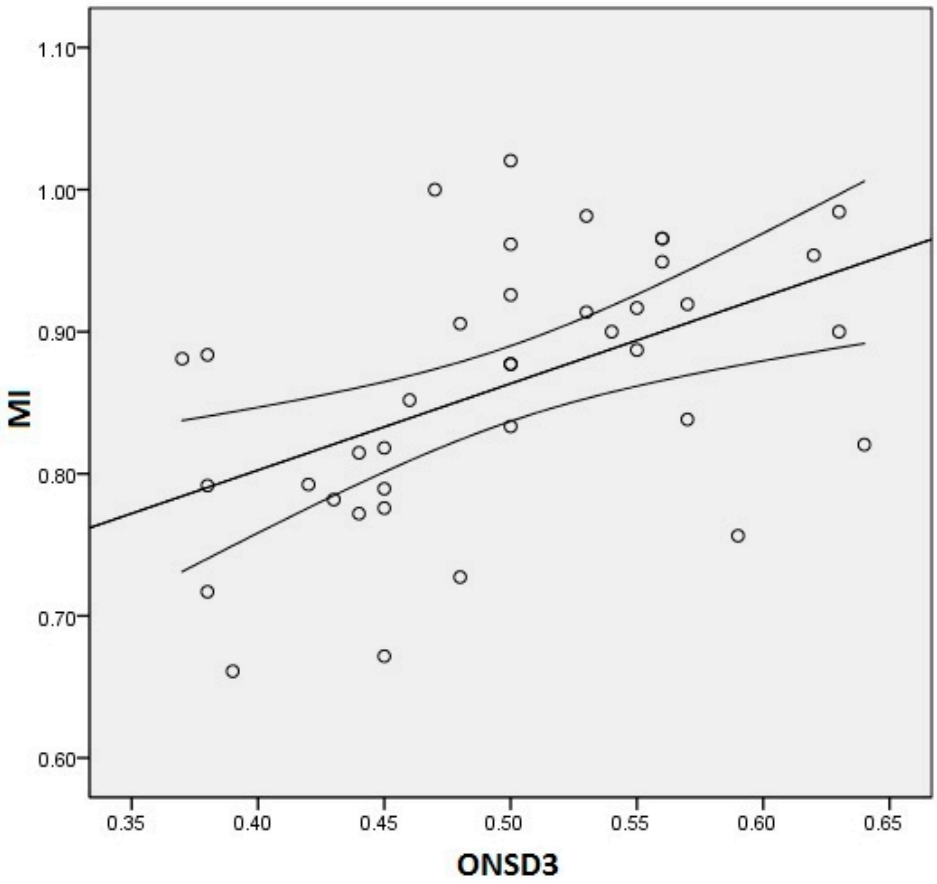

Figure 3. Correlation between MI and ONSD3. Significant correlation between Myelination Index (MI) and optic nerve sheath diameter measured at 3 mm from the eyeball (ONSD3). (r = 0.499; p = 0.001).

4. Discussion and Conclusions

In a comparative, unblinded, cross-sectional study of a relapse-free MS population and matched healthy controls we found broad variation in ONSD, which proved to be significantly smaller in the MS group, at both 3 and 5 mm from the eyeball. Furthermore, ONSD at 5 mm from the eyeball proved to be significantly smaller in the SP group than the RR group. In contrast, the gap between ONSD at 3 mm in the two groups was not statistically significant.

This finding was not seen in RR patients with a mean EDSS of 2.0 compared with transitional patients who have a mean EDSS of 3.7.

These RR patients with a mean EDSS of 2.0 had a higher mean ONSD3 (0.53 cm) and MI (0.90) than the transitional group (0.48 cm and 0.84), (p = 0.050 and p = 0.050 respectively). These data demonstrate that MS phenotypes are characterized by readily detectable degrees of ON atrophy and neuropathy. Therefore, we can state that the major contributors to ON neuropathy are axonal loss and demyelination. These findings are in accordance with the common interpretation of optical coherence tomography (OCT) data, which is that retinal atrophy in multiple sclerosis reflects loss of retinal ganglion cells and their axons [17].

Based on different physical principles, OCT and ONSD are not complementary methods, but reflect structural aspects of separated but highly correlated organs: the retina and the ON. To our knowledge, no published studies have explored the degree of correlation and concordance between the two methods. Further investigations are warranted. Specifically, it should be stressed that in the literature there is no evidence of correlation between age and ONSD, as well as height and body mass index [18]. Thus, despite the significantly greater age of the SPMS patients, the differences in ONSD with respect to the RRMS group are due to disease activity and disease duration.

Moreover, we demonstrated a linear correlation between the MI and ONSD3 among the MS population, but not between the MI and ONSD5. This means that neurodegeneration in the ON begins early in RRMS and reaches a plateau during the transitional phase. However, it remains stable and mild throughout the patient's life, even in the SP phase. On the other hand, the inflammatory demyelination process begins during the RR phase and continues over time during the SP phase, where it is preponderant.

In addition, as expected, we found lower PGMv and TBv as well as higher T1LL, T2LL, EDSS (and its sensitive, pyramidal, cerebellar, brain stem and sphincteric sub-scores), age, and DD in the SP group than in the RR group, but the mean MI was not found to be statistically different between the two groups.

The latter finding can have only one explanation: subclinical ON demyelination during the natural progression of MS. For this reason, although the absolute size of the ON is lower in MS than in healthy controls, and the ONSD measured at 5 mm from the eyeball is higher in the RR patients than in the SP group, the relative amount of myelin can raise the MI, reducing its statistical significance.

In contrast, at 3 mm from the eyeball, the myelin coating is significantly thinner, so the axonal loss or shrinkage already detected in this segment in comparison to the healthy controls is mild and distributed equally between the RR and the SP patients. This explanation is in accordance with previous observations regarding the brain lesion re-myelination process, the effectiveness of which is largely dependent on the subjective characteristics of the MS patient, including genetics, age, and DD [19,20]. For the same reason, the MI does not correlate with the clinical or neurophysiological variables, nor can it distinguish RR from SP patients, as demonstrated by the ROC analysis.

However, the similarity statistics blindly identified two groups, one with MI^H and another with MI^L. In the MI^H group, patients with a mean EDSS of 2.0 and DD $\leq$ 38.29 y form a cluster corresponding to the RR phenotype, whereas in the MI^L group, patients with a mean EDSS of 3.7 and DD $\geq$ 45.47 y form a cluster corresponding to the transitional phenotype. In all these cases we found the distances between the centres of each variable, including the MI, to be statistically significant. This means that the MI is statistically associated with a qualitative state variable, not with a continuous quantitative variable expressible as a number, for example the T1LL, DD, etc. In physiopathological terms, in the transitional phase of MS, demyelination is not yet advanced enough to modify the MI.

In contrast, in clinical terms, we can state that the MI is associated with either an RR or a transitional clinical phenotype, depending on whether it exceeds the cut-off of 0.84. However, this association becomes stringent only if the MI is supported by at least one of the following: DD, age, T1LL, T2LL, P100A, P100L. This means that subclinical axonal loss, as well as de/re-myelination, can vary subjectively. However, when considered together with another patient-specific neurophysiological parameter, it contributes to establishing the clinical phenotype.

Specifically, a patient with an MI of 0.90 with ONSD3 $\geq$ 0.53 or ONSD5 $\geq$ 0.59 will belong to the RR group, while an MI of 0.84 with an ONSD3 ranging from 0.46 to 0.48 indicates the transitional group. Finally, an MI of < 0.83 with ONSD5 $\leq$ 0.55 or ONSD3 $\leq$ 0.46 indicates the SP group (Figure 4).

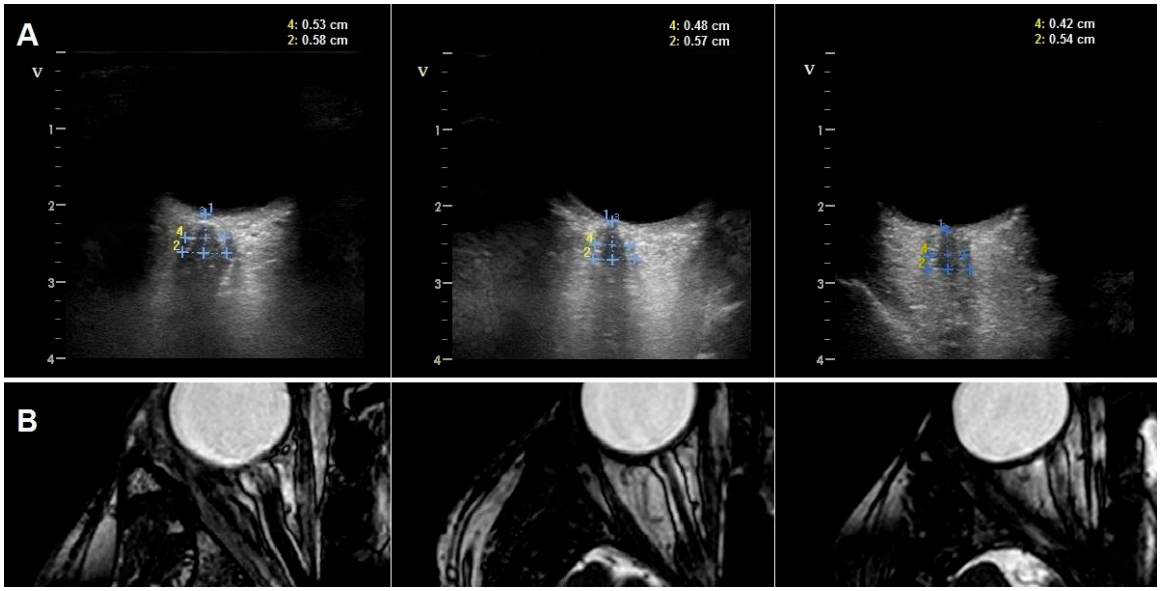

Figure 4. Transbulbar B-mode sonography and MRI. (**A**) Transbulbar B-mode sonography and (**B**) magnetic resonance images of the optic nerve sheath diameter (ONSD) of (from left to right) relapsing remitting, transitional, and secondary progressive multiple sclerosis patients. The distance between the external borders of the hyper-echoic area surrounding the optic nerve was quantified as ONSD. Lines 4 and 2 indicate ONSD at 3 and 5 mm from the eyeball, respectively. All magnetic resonance images refer to T2/T1 bFFE sequences, acquired with SENSE (Sensitivity Encoding) Head 8 channels. Note the progressive decrease in ONSD and the MI (0.91; 0.84; 0.77) moving through three different phenotypes of disease. MI Myelination index; MRI Magnetic resonance imaging.

In our study population, these conditions correctly clustered the subgroups with ≈90% accuracy. Considering these physiopathological elements as a whole, we found significant similarities between the ON and the brain: early subclinical involvement; co-existing inflammatory demyelination with possible exacerbation phases and chronic axonal loss, leading to progressive nerve atrophy; and correlations between ONSD and clinical/paraclinical impairment. Coherently, TBS-detected ONSD reflects the demyelination induced by inflammation, but not the inflammation itself that is underlying pathological process. These elements, numerous and consistent with each other, are supported by statistics and therefore, in our view, are not mere coincidence. These non-casual similarities make the ON a "long brain" and a useful clinical model of disease.

The limitation of the study is that the sonographer was unblinded concerning the clinical conditions. This bias was in part offset by calculating the COV, which confirmed the reliability of the measurements. Another issue is that the measurements are very small in size, although we should consider the wider context of the study. Specifically, the high sensitivity of the B-mode system, accurate to a tenth of a millimetre with a very low standard deviation of measurements, ensures the statistical significance of even apparently small differences between compared means. The same consideration applies to normative data, according to which an ONSD of 5.4 ± 0.6 mm is considered normal, while $\geq 6.3 \pm 0.6$ mm is considered predictive of elevated intracranial pressure [21]. As for the papilla, a disc elevation of 1.2 ± 0.3 mm is considered strongly indicative of papilloedema [1]. Moreover, based on sub-millimetric measurement, the high-resolution B-mode system also provides an appropriate evaluation of the intima-media thickness as a marker of atherosclerosis [22]. Finally, in this paper we have not considered primary progressive MS (PPMS) and neuromyelitis optica (NMO) as comparison groups with respect to our MS study population. These interesting evaluations are missing in both cases, but we must consider that these are nosografically isolated pathologies not evolving from other demyelinating subtypes and requiring specific diagnostic guidelines. In our opinion, PPMS and NMO deserve a separate treatment, considering also the absence of literature data on TBS.

To summarize, the neuro-sonographic study of chronic optic neuropathy in terms of ONSD highlights lower values at 5 mm in the SP group, due to the lack of myelin repair, subclinical demyelination, and axonal loss. The latter phenomenon is preponderant during this stage of the disease, given that there is no difference between the RR and SP groups regarding the ONSD at 3 mm from the eyeball. Therefore, involvement of the ON can be described as "mild" in ARON-free MS patients. Finally, the MI can add a number of physiopathological elements linked to individual MS patients, meaning that it is also useful in defining their clinical phenotype.

On these pathological bases, it can be stated that B-mode sonography represents a useful technique for the documentation of ON atrophy. This application could have clinically important implications in determining the dissemination in space (DIS) or time (DIT) of the pathological process in MS, especially if the diagnostic guidelines incorporate the ON as an MS typical region, as recently proposed by the MAGNIMS (magnetic resonance imaging in multiple sclerosis) group [23]. In this case, TBS could be included in the routine clinical practice of the diagnostic iter of MS. Traslated in clinical terms, our data also suggest a valuable role of B-mode sonography in the clinical phenotyping of MS patients. Given that therapeutic management of MS is closely related subtype individuation, it follows that TBS could provide an objective instrumental criterion for personalized therapeutic choice in MS.

Author Contributions: R.D.M. has made substantial contributions to conception and design, acquisition of data, analysis, and interpretation of data. S.O. has been involved in drafting the manuscript and revising it critically for important intellectual content. A.C. and P.S. have contributed to acquisition and analysis of data. S.P. and R.S. have given final approval of the version to be published. A.D.D. agrees to be accountable for all aspects of the work in ensuring that questions related to the accuracy and integrity of any part of the work are appropriately investigated and resolved.

Funding: This research received no external funding.

Acknowledgments: We thank our multiple sclerosis nurses, Valeria Piccinni and Donata Branca, for technical support and the local ethics committee for approval.

Conflicts of Interest: The authors declare no conflict of interest.

References

1. Bauerle, J.; Lochner, P.; Kaps, M.; Nedelmann, M. Intra- and interobsever reliability of sonographic assessment of the optic nerve sheath diameter in healthy adults. *J. Neuroimaging* **2012**, *22*, 42–45. [CrossRef] [PubMed]
2. Bauerle, J.; Schuchardt, F.; Schroeder, L.; Egger, K.; Weigel, M.; Harloff, A. Reproducibility and accuracy of optic nerve sheath diameter assessment using ultrasound compared to magnetic resonance imaging. *BMC Neurol.* **2013**, *13*, 187. [CrossRef] [PubMed]
3. Bauerle, J.; Nedelmann, M. Sonographic assessment of the optic nerve sheath in idiopathic intracranial hypertension. *J. Neurol.* **2011**, *258*, 2014–2019. [CrossRef] [PubMed]
4. Rehman, H.; Khan, M.S.; Nafees, M.; Rehman, A.U.; Habib, A. Optic Nerve Sheath Diameter on Sonography in Idiopathic Intracranial Hypertension Versus Normal. *J. Coll. Phys. Surg. Pak.* **2016**, *26*, 758–760.
5. Merola, A.; Rosso, M.; Romagnolo, A.; Peci, E.; Cocito, D. Peripheral Nerve Ultrasonography in Chronic Inflammatory Demyelinating Polyradiculoneuropathy and Multifocal Motor Neuropathy: Correlations with Clinical and Neurophysiological Data. *Neurol. Res. Int.* **2016**, *2016*, 9478593. [CrossRef] [PubMed]
6. Lochner, P.; Leone, M.A.; Coppo, L.; Nardone, R.; Zedde, M.L.; Cantello, R.; Brigo, F. B-mode transorbital ultrasononography for the diagnosis of acute optic neuritis. A systematic review. *Clin. Neurophysiol.* **2016**, *127*, 803–809. [CrossRef] [PubMed]
7. Stefanović, I.B.; Jovanović, M.; Krnjaja, B.D.; Veselinović, D.; Jovanović, P. Influence of retrobulbar neuritis and papillitis on echographically measured optic nerve diameter. *Vojnosanit. Pregl.* **2010**, *67*, 32–35. [CrossRef] [PubMed]
8. De Masi, R.; Orlando, S.; Conte, A.; Pasca, S.; Scarpello, R.; Spagnolo, P.; Muscella, A.; De Donno, A. Transbulbar B-Mode Sonography in Multiple Sclerosis: Clinical and Biological Relevance. *Ultrasound Med. Biol.* **2016**, *42*, 3037–3042. [CrossRef] [PubMed]

9. Costello, F.; Coupland, S.; Hodge, W.; Lorello, G.R.; Koroluk, J.; Pan, Y.I.; Freedman, M.S.; Zackon, D.H.; Kardon, R.H. Quantifying axonal loss after optic neuritis with optical coherence tomography. *Ann. Neurol.* **2006**, *59*, 963–969. [CrossRef] [PubMed]
10. Hayreh, S.S. Structure of the optic nerve. In *Ischemic Optic Neuropathies*; Springer: Berlin/Heidelberg, Germany, 2011; Volume 12, p. 456.
11. Minagar, A.; Barnett, M.H.; Benedict, R.H.; Pelletier, D.; Pirko, I.; Sahraian, M.A.; Frohman, E.; Zivadinov, R. The thalamus and multiple sclerosis: Modern views on pathologic, imaging, and clinical aspects. *Neurology* **2013**, *80*, 210–219. [CrossRef] [PubMed]
12. Muller, M.; Esser, R.; Kotter, K.; Voss, J.; Muller, A.; Stellmes, P. Third ventricular enlargement in early stages of multiple sclerosis is a predictor of motor and neuropsychological deficits: A cross-sectional study. *BMJ Open* **2013**, *3*, e003582. [CrossRef] [PubMed]
13. Stadelmann, C.; Wegner, C.; Bruck, W. Inflammation, demyelination, and degeneration—Recent insights from MS pathology. *Biochim. Biophys. Acta* **2011**, *1812*, 275–282. [CrossRef] [PubMed]
14. Gupta, S.; Gupta, G.; Deshpande, V. Visual evoked potentials: Impact of age, gender, head size and BMI. *Int. J. Biomed. Adv. Res.* **2016**, *7*, 22–26. [CrossRef]
15. Miller, D.H.; Barkhof, F.; Berry, I.; Kappos, L.; Scotti, G. Magnetic resonance imaging in monitoring the treatment of multiple sclerosis: Concerted action guidelines. *J. Neurol. Neurosurg. Psychiatry* **1991**, *54*, 683–688. [CrossRef] [PubMed]
16. Kurtzke, F. Rating neurologic impairment in multiple sclerosis: An expanded disability status scale (EDSS). *Neurology* **1983**, *33*, 1444–1452. [CrossRef] [PubMed]
17. Green, A.J.; McQuaid, S.; Hauser, S.L.; Allen, I.V.; Lyness, R. Ocular pathology in multiple sclerosis: Retinal atrophy and inflammation irrespective of disease duration. *Brain* **2010**, *133*, 1591–1601. [CrossRef] [PubMed]
18. Asghar, A.; Hashmi, M.; Hussain, A. Optic nerve sheath diameter evaluated by transorbital sonography in healthy volunteers from Pakistan. *Anaesth. Pain Intensive Care* **2015**, *19*, 282–286.
19. Ligon, K.L.; Fancy, S.P.J.; Franklin, R.J.M.; Rowitch, D.H. Olig gene function in CNS development and disease. *Glia* **2006**, *54*, 1–10. [CrossRef] [PubMed]
20. Adamo, A.M. Nutritional factors and aging in demyelinating diseases. *Genes Nutr.* **2014**, *9*, 360. [CrossRef] [PubMed]
21. Geeraerts, T.; Launey, Y.; Martin, L.; Pottecher, J.; Vigué, B.; Duranteau, J.; Benhamou, D. Ultrasonography of the optic nerve sheath may be useful for detecting raised intracranial pressure after severe brain injury. *Intensive Care Med.* **2007**, *33*, 1704–1711. [CrossRef] [PubMed]
22. Lorenz, M.W.; Markus, H.S.; Bots, M.L.; Rosvall, M.; Sitzer, M. Prediction of clinical cardiovascular events with carotid intima-media thickness: A systematic review and meta-analysis. *Circulation* **2007**, *115*, 459–467. [CrossRef] [PubMed]
23. Filippi, M.; Rocca, M.A.; Ciccarelli, O.; De Stefano, N.; Evangelou, N.; Kappos, L.; Rovira, A.; Sastre-Garriga, J.; Tintorè, M.; Frederiksen, J.L.; et al. MRI criteria for the diagnosis of multiple sclerosis: MAGNIMS consensus guidelines. *Lancet Neurol.* **2016**, *15*, 292–303. [CrossRef]